

UCSF

UC San Francisco Previously Published Works

Title

Blockade of current through single calcium channels by trivalent lanthanide cations. Effect of ionic radius on the rates of ion entry and exit.

Permalink

<https://escholarship.org/uc/item/7q83g0wq>

Journal

The Journal of general physiology, 95(4)

ISSN

0022-1295

Author

Lansman, JB

Publication Date

1990-04-01

DOI

10.1085/jgp.95.4.679

Peer reviewed

Blockade of Current through Single Calcium Channels by Trivalent Lanthanide Cations

Effect of Ionic Radius on the Rates of Ion Entry and Exit

JEFFRY B. LANSMAN

From the Department of Pharmacology, School of Medicine, University of California, San Francisco, California 94143-0450

ABSTRACT Currents flowing through single dihydropyridine-sensitive Ca^{2+} channels were recorded from cell-attached patches on C2 myotubes. In the presence of dihydropyridine agonist to prolong the duration of single-channel openings, adding micromolar concentrations of lanthanum (La), cerium (Ce), neodymium (Nd), gadolinium (Gd), dysprosium (Dy), or ytterbium (Yb) to patch electrodes containing 110 mM BaCl_2 caused the unitary Ba^{2+} currents to fluctuate between fully open and shut states. The kinetics of channel blockade followed the predictions of a simple open channel block model in which the fluctuations of the single-channel current arose from the entry and exit of blocking ions from the pore. Entry rates for all the lanthanides tested were relatively insensitive to membrane potential, however, exit rates depended strongly on membrane potential increasing $\sim e$ -fold per 23 mV with hyperpolarization. Individual lanthanide ions differed in both the absolute rates of ion entry and exit: entry rates decreased as cationic radius decreased; exit rates also decreased with cationic radius during the first part of the lanthanide series but then showed little change during the latter part of the series. Overall, the results support the idea that smaller ions enter the channel more slowly, presumably because they dehydrate more slowly; smaller ions also bind more tightly to a site within the channel pore, but lanthanide residence time within the channel approaches a maximum for the smaller cations with radii less than or equal to that of Ca^{2+} .

INTRODUCTION

A wide variety of multivalent cations block current flow through voltage-gated calcium channels. Blocking ions compete with Ca^{2+} for a channel binding site and inhibit the flow of permeant ions because their overall mobility through the channel

Address reprint requests to Dr. Jeffry B. Lansman, Department of Pharmacology, School of Medicine, University of California, San Francisco, CA 94143-0450.

is low (Hagiwara and Takahashi, 1967; Hagiwara, 1975; Hagiwara and Byerly, 1981). Blocking potencies range from very strong blockers such as La^{3+} and Cd^{2+} , which completely inhibit Ca^{2+} channel current at micromolar concentrations, to relatively weak blockers such as Co^{2+} and Mg^{2+} , which are effective blockers only at millimolar concentrations.

Resolution of the individual steps of blocking and unblocking at the single-channel level helped clarify the mechanism by which metal ions block current through Ca^{2+} channels (Lansman et al., 1986). The blocking actions of multivalent cations appear as discrete fluctuations of the single-channel current between the fully open and blocked states produced as the blocker enters and exits the channel pore (cf. Neher and Steinbach, 1978; Fukushima, 1982). The kinetics of the individual steps of blockade vary with membrane potential in such a way as to suggest that the blocking site resides within the pore and that the effect of voltage is to alter the distribution of the charged blocking particle within the membrane field (Woodhull, 1973).

Divalent cations such as Cd^{2+} , Co^{2+} , Mn^{2+} , and Mg^{2+} , which are widely used to block Ca^{2+} channel currents, vary considerably in the absolute rates of entry into the channel and exit from the channel pore (Lansman et al., 1986). Cd^{2+} enters the channel rapidly with a rate approaching that of diffusion in free solution and binds tightly to the channel. On the other hand, Mg^{2+} enters the channel several orders of magnitude more slowly, presumably because it is smaller and binds water tightly and so dehydrates more slowly (Dieber et al., 1969; Hague, 1977). However, Mg^{2+} binds less tightly than Cd^{2+} to the intrapore site and so spends less time within the channel. Other metal ions that block Ca^{2+} channels fall more or less within these extreme rates of ion entry and exit.

Ion transport through membrane channels is thought to involve removal of water molecules from the primary hydration sphere of the permeant ion with step-wise substitution of the water molecules by pore ligands (see Hille, 1984). Cationic radius is an important variable that determines the rates of ion interactions with water molecules in solution and with ion binding sites of proteins (Tam and Williams, 1985). Because many of the metal ions that inhibit Ca^{2+} channel current vary in chemical properties such as coordination number and polarizability as well as ionic radius, it is difficult to determine how differences in ion size influence the individual steps of ion transfer through Ca^{2+} channels.

The trivalent lanthanide cations are well suited for studying the effects of ionic radius on ion interactions with Ca^{2+} binding sites of proteins. Lanthanides have ionic radii and coordination numbers that are similar to Ca^{2+} and, like Ca^{2+} , prefer to bind to oxygen donor groups (Nieboer, 1975; Martin and Richardson, 1979; dos Remedios, 1981; Williams, 1982). Because the lanthanides have ionic radii which vary by $\sim 0.01 \text{ \AA}$ along the series, they provide an opportunity to investigate how ion size differences influence the individual steps of ion entry and exit from the Ca^{2+} channel pore. A preliminary report describing this work has been published as an abstract (Lansman, 1989).

MATERIALS AND METHODS

Culture of C2 Muscle Cells

C2 cells were originally isolated from adult mouse skeletal muscle by Yaffe and Saxel (1977) and were cultured following the procedure of Inestrosa et al. (1983). Myoblasts were grown

in plastic tissue culture dishes in Dulbecco's modified Eagle's medium containing 20% fetal calf serum and 0.5% chick embryo extract (growth medium) at 37°C in an incubator containing 95% air/5% CO₂. Cells were passaged at ~75% confluency every 2–3 d to maintain stocks of growing cells. The generation time is roughly 14 h.

Differentiated myotubes were prepared by plating myoblasts at 5,000–10,000 cells per cm² in growth medium. When the plated cells reached ~75% confluence, the culture medium was replaced with Dulbecco's modified Eagle's medium containing 2% calf serum (fusion medium). Reducing the amount of serum in the culture medium is a sufficient stimulus to cause myoblasts to leave the proliferative phase and begin to fuse and form multinucleated myotubes (Linkhart et al., 1981). Half of the culture media was replaced with fresh media every 3 d and the night before experiments. This procedure produces cultures of cells that differentiate in vitro in well-defined, morphologically identifiable stages. Myotubes could be maintained in culture for up to 3 wk, however, most experiments were done on myotubes less than 1 wk old.

Electrophysiological Methods

Unitary Ca²⁺ channel activity was recorded from cell-attached patches on the surface of myotubes with the technique described by Hamill et al. (1981). Patch electrodes were pulled in two steps from Boralex hematocrit pipettes (Rochester Scientific Co., Rochester, NY) the shanks were coated with Sylgard (Dow Corning Corp., Midland, MI) to within ~1 mm of the tip, and the tips were heat-polished with a microforge. Patch electrodes had resistances of 2–4 MΩ when filled with 110 mM BaCl₂ and immersed in an isotonic potassium-aspartate bathing solution. All experiments were done at room temperature (~21–23°C).

Current signals were recorded with a List EPC-7 patch-clamp amplifier, filtered with an eight-pole Bessel filter (–3 dB at 1 kHz) and digitized at 5 kHz. Unitary Ca²⁺ channel currents evoked by test pulses were stored directly on the laboratory computer (PDP 11/73; Indec Systems, Sunnyvale, CA). At the time of recording, analog capacity compensation was used. Before analysis, the remaining capacity and leakage current was removed by subtracting a template formatted by averaging current records lacking channel openings from individual records with channel activity.

Solutions

The patch electrode filling solution contained 110 mM BaCl₂, 10 mM glucose, and 10 mM HEPES. The pH was adjusted to 7.5 by adding tetraethylammonium hydroxide (TEA-OH). Lanthanides (Aldrich Chemical, >99.9% purity) were added to the electrode filling solution either directly as the chloride salt or as an aliquot from a 10-mM stock solution of the chloride salt.

Lanthanides act as acids in aqueous solution. Hydrolysis of La³⁺ produces La(OH)²⁺ and higher valence species (Biedermann and Ciavatta, 1961). The percentages of divalent hydroxide in solutions of the various lanthanides at pH 7.5 calculated with the association constants given in Smith and Martell (1976) for 0.5 M ionic strength at 25°C are 2, 7, 8, 13, and 19% for La, Nd, Gd, Dy, and Yb, respectively (the association constant for Ce is not given). Values of lanthanide hydrolysis constants given by other sources can vary by several orders of magnitude and the uncertainties associated with their determination has been attributed to lanthanide polymerization reactions which occur in solution. A much larger percentage of the charged lanthanide species in the experimental solution may be the divalent hydroxide, which may account for the similar dependence on membrane potential of the exit rates for Cd and La found in a previous study (Lansman et al., 1986). This issue of the valence of the blocking particle is taken up further in the Discussion. Lanthanides also bind to physiological buffers, however, values for these stability constants have not been reported. Binding of lanthanides to the electrode glass and to charged groups at the membrane surface introduces additional

uncertainty as to the concentration of free cation at the membrane surface (dos Remedios, 1981). Because the concentration of free lanthanide ions at the membrane surface is not known with any certainty under the experimental conditions, the absolute values of the entry rate constants must be considered as only an approximation to their true values.

The bathing solution contained 150 mM potassium aspartate, 5 mM MgCl_2 , 10 mM K-EGTA, 10 mM HEPES, and the pH was adjusted to 7.4 with TEA-OH. An isotonic K^+ bathing solution was used to zero the cell's resting potential so that the patch membrane potential would be identical to the command voltage applied to the amplifier (Hess et al., 1986). This assumption was justified in most experiments because the unitary current-voltage (I - V) relation, measured after excising the patch at the end of the experiment, was not different from that measured during the course of the experiment. In some experiments, the I - V relation was shifted to more negative potentials after patch excision. The maximum shift observed indicated a voltage error of ~ 10 mV. To minimize the error introduced by uncontrolled shifts in membrane potential, blocking kinetics were analyzed from experiments in which the unitary current at 0 mV was 0.7–0.9 pA. Indicated patch potentials could be in error by ~ 10 mV. The K^+ -aspartate bathing solution produced no visibly detectable signs of cell deterioration.

Analysis of Channel Blockade

The activity of single Ca^{2+} channels can be recorded from the surface membrane of skeletal muscle cells from the C2 cell line, although openings are brief and occur rarely in response to voltage steps to 0 mV. The cumulative latency to first opening does not reach a plateau until >200 ms after the onset of a voltage pulse to 0 mV, which indicates that the activation kinetics are quite slow (Franco, A., and J. B. Lansman, unpublished observation). These channels have a unitary conductance of 12–16 pS in the presence of 110 mM BaCl_2 and, like the larger conductance channel in cardiac muscle, dihydropyridine agonists prolong the mean open time (Hess et al., 1984).

In these experiments, the dihydropyridine agonist (+)-202-791 (Sandoz Ltd., Basel, Switzerland) was used to increase the duration of channel openings. Even in the presence of dihydropyridine agonist, however, channels rarely opened in response to voltage steps to 0 mV. Applying strong depolarizing prepulses ($\sim +30$ to $+70$ mV) fully activated channels and allowed channel openings to be detected after repolarizing the patch to the test potential as single-channel tail currents (cf. Hoshi and Smith, 1987). The prepulse protocol extended the voltage range at which single channel events could be detected to potentials significantly more negative than the threshold for activation.

Fig. 1 shows the pattern of Ca^{2+} channel activity after strong depolarizing prepulses recorded from cell-attached patches on C2 myotubes. Cells were bathed in an isotonic K^+ -aspartate solution containing ~ 1 μM of the dihydropyridine agonist (+)-202-791. In this figure, the membrane potential was stepped from a holding potential of -70 mV to the prepulse level of $+50$ mV for 224 ms before returning the potential to the test level of -10 mV. The records in Fig. 1 represent consecutive current responses evoked by the voltage protocol (*top*) delivered once every 3 s. Channel activity occurred in a characteristic pattern that included sweeps in which the channel remained open during the entire test pulse, sweeps without openings, and occasional sweeps with short openings. Because in most sweeps, channels were open after returning the membrane potential from the prepulse level to the test pulse and remained open throughout the test pulse (Fig. 1, sweeps 1 and 3), no attempt was made to measure the mean open time in the absence of blocking ion.

Blockages produced by smaller lanthanides (Nd through Yb) at 0 mV were relatively long compared with the test pulse duration (see Fig. 6). Openings during the test pulse could have come from different channels even though simultaneous openings were not observed. This

problem was minimized by analyzing kinetics from experiments in which the overall probability of channel opening was low as indicated by a high proportion of blank sweeps and rejecting sweeps where more than one channel was open during the pulse, as indicated by the presence of overlapping channel events. At test potentials more negative than 0 mV, identifying individual bursts of openings arising from the blocking and unblocking transitions of a single channel was more reliable because the blocked times became shorter and the channel closing rate increased: virtually all of the closings could be attributed to blocking events because blocking and unblocking were fast relative to channel gating.

To interpret the interaction of lanthanide cations with the Ca^{2+} channel, a simple open-channel block model, in which a closed state, an open state, and a blocked state are arranged

110mM Ba - Control

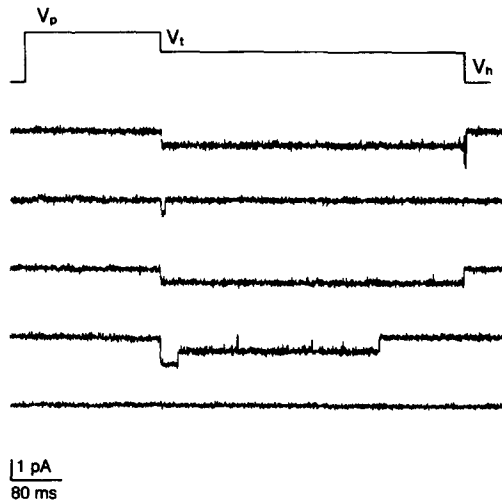
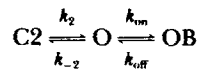


FIGURE 1. Unitary Ba^{2+} currents recorded from cell-attached patches on the surface membrane of C2 myotubes. Channel openings were evoked by the pulse paradigm shown at the top of the figure. The patch was depolarized from a holding potential of -70 to $+50$ mV for ~ 224 ms after which the potential was stepped down to -10 mV for ~ 500 ms before returning to the holding potential. Records were corrected for linear leak and capacity currents as described in Materials and Methods. The cell was bathed in an isotonic K^+ aspartate solution to zero the cell's resting potential. The patch electrode contained 110 mM BaCl_2 .

sequentially (Armstrong, 1966, 1969; Neher and Steinbach, 1978) adequately described the main kinetic features of channel blockade:



where the rate constants k_2 and k_{-2} represent the kinetic constants that govern the voltage-dependent opening of the Ca^{2+} channel from the last closed state C2, and k_{on} and k_{off} describe the rates of entry into and exit from the pore, respectively. The blocking (or entry) rate constant, k_{on} , is also a function of the concentration of both the blocking ion and permeant ion (Lansman et al., 1986). The rate constants in the model are related to the experimentally measured open and blocked times as

$$1/\tau_o = k_{-2} + k_{\text{on}}[\text{Ln}]_o \quad (1)$$

$$1/\tau_b = k_{\text{off}} \quad (2)$$

Error in the concentration of free lanthanide cation would not be expected to alter blocked times. The error in measured second-order rate coefficients was estimated by rotat-

ing the least-squares regression line through the experimental points, keeping the point at the ordinate fixed, to get a value for the minimum and maximum slope at the extreme values of the data points.

RESULTS

Kinetic Analysis of La Block of Ba^{2+} Currents

Fig. 2 shows recordings from three separate cell-attached patches in which the patch electrode contained 5, 25, or 100 μM LaCl_3 . When La was included in the patch electrode, the unitary currents carried by 110 mM Ba^{2+} flickered between the fully open and fully closed (blocked) levels. Increasing the concentration of La in the electrode increased the flickering of the single-channel current without measurably reducing the single-channel conductance, suggesting that La falls within the class of slow blockers that produces discrete blocking events.

110mM Ba

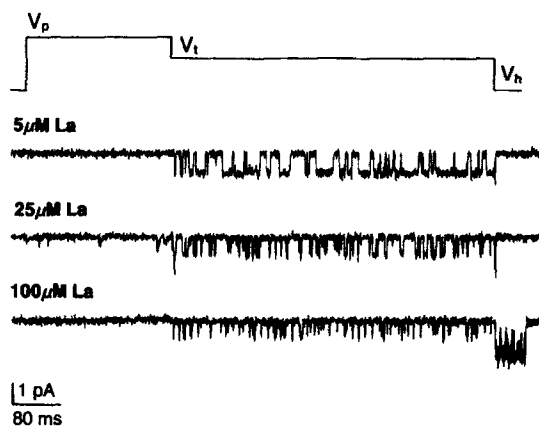


FIGURE 2. Block of unitary Ba^{2+} currents in the presence of different concentrations of La. Records are from three different cells in which the patch electrode contained 110 mM $BaCl_2$, to which was added the indicated concentration of LaCl_3 . The test potential was 0 mV. Cells N03B, N05E, N07a.

Histograms were constructed from the measurements of open and shut periods. Fig. 3 A shows histograms of open and shut times obtained from the La blocking experiments shown in Fig. 2. As predicted by the blocking model, single exponentials fit histograms of both open and shut periods, suggesting the existence of a single open and a single blocked state. The effect of increasing the concentration of La in the patch electrode on the kinetics of blockade can be seen in Fig. 3 A by comparing the time constants obtained from the exponential fits with the histograms: mean open times decreased as the concentration of La in the electrode solution was increased from 7.7 ms with 5 μM La in the electrode to 0.7 ms with 100 μM La. Mean blocked times, on the other hand, were relatively insensitive to changing the concentration of La in the patch electrode. Both of these observations are consistent with the blocking model which predicts a concentration-dependent blocking rate and a concentration-independent rate of unblocking.

Fig. 3 B (*top*) shows the inverse of the mean open time (entry rate) plotted as a

function of the concentration of La in the patch electrode. The inverse of the mean open time varied linearly with the concentration of La. The slope of the regression line was $\sim 14 \times 10^6 \text{ M}^{-1}\text{s}^{-1}$, which is the second-order rate coefficient for La entry into the channel. Fig. 3 *B* (bottom) confirms that the inverse of the mean blocked time (exit rate) did not vary with the concentration of La in the patch electrode.

Voltage Dependence of La Block of Ba^{2+} Currents

Studies of La block of single dihydropyridine-sensitive Ca^{2+} channels in heart muscle showed that hyperpolarizing the membrane potential reduced the duration of

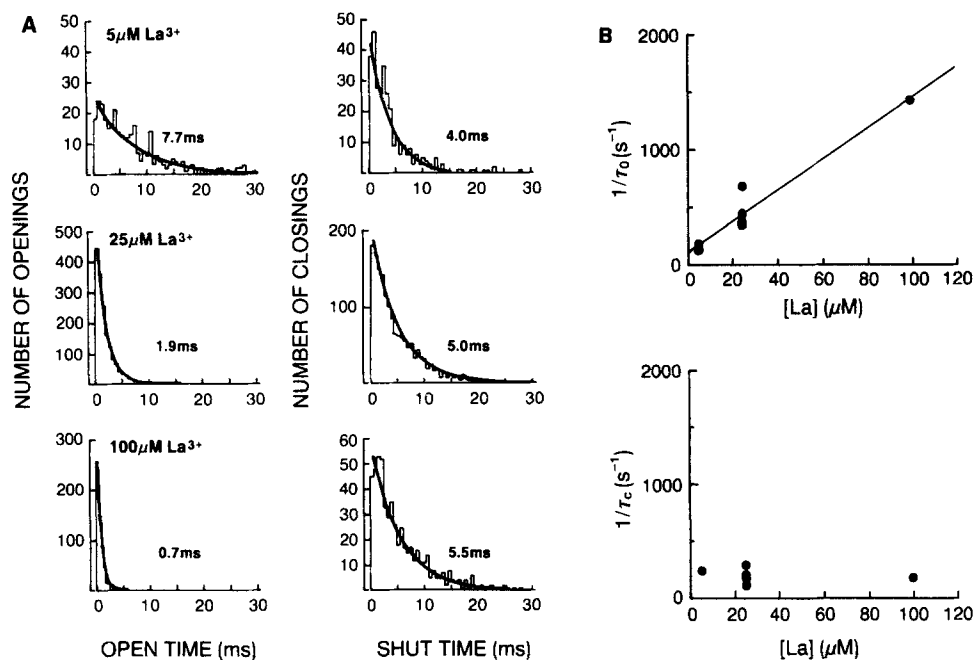


FIGURE 3. Kinetic analysis of block of unitary Ba^{2+} currents by La. (A) Histograms of open and shut (blocked) times obtained from the experiments from which the records in Fig. 2 were taken. The histograms plot the numbers of openings (*left*) and closings (*right*) of the durations indicated. The smooth curve is drawn to a single exponential with the indicated time constant. (B) Inverse of the mean open time (k_{on}) and mean blocked time (k_{off}) plotted as a function of $[\text{La}]_o$. Each point is from a different patch. The straight line is the least-squares regression with a y-intercept of 1/17 ms and a slope of $14 \times 10^6 \text{ M}^{-1}\text{s}^{-1}$ ($r = 0.97$).

the blockages produced by La (Lansman et al., 1986). The experiments in this section examined the effects of membrane potential on the kinetics of La block of the smaller conductance skeletal muscle Ca^{2+} channel.

The effects of changing the membrane potential on the pattern of block produced by La are shown in Fig. 4. The records in Fig. 4 are from a single experiment in which the patch electrode contained 25 μM La. The recordings were made after

repolarizing the membrane potential to either 0, -20 , or -40 mV after a strong depolarizing prepulse. At the end of the test pulse, the patch potential was returned to the holding level of -80 mV.

The effect of membrane potential on the pattern of block can be seen in the records. Closings within a burst become shorter as the test potential became more negative. This can be explained by membrane hyperpolarization reducing the dwell time of La within the channel. The effect of membrane potential on the histograms of open and blocked times for this experiment is shown in Fig. 5 A. As expected for a single open and a single blocked state, the histograms are well fit with a single exponential over a range of membrane potentials. As can be seen from the histograms, blocked times decreased from 5.0 ms at 0 mV to 0.7 ms at -40 mV, while open times were relatively insensitive to membrane potential.

The inverse of the mean open and blocked times for a range of membrane potentials ($+10$ to -40 mV) is plotted against membrane potential on a semilogarithmic scale in Fig. 5 B. The mean blocked time depended strongly on membrane potential.

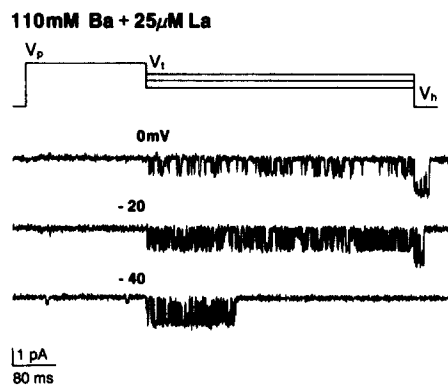


FIGURE 4. Effect of changing the test potential on the block of unitary Ba^{2+} currents by La. A prepulse to $+70$ mV was followed by test pulses to 0, -20 , and -40 mV. The holding potential was -90 mV. The tail current at the end of the first record is the current produced after returning the patch potential from the test potential of 0 mV to -90 mV. $[\text{La}]_o = 25 \mu\text{M}$. Cell N05e.

For all of the experiments with La, the exit rate ($1/\tau_b$) changed $\sim e$ -fold per 20 mV change in membrane potential ($n = 5$, $r^2 = 0.94$). On the other hand, the inverse of the mean open time showed little dependence on membrane potential. This pattern of voltage dependence is a general characteristic of channel blockade produced by lanthanide cations as shown in more detail below. From the experiment shown in Fig. 5 and others like it, it is concluded that block by La depends on membrane potential in such a manner that hyperpolarization reduces the time La spends within the channel.

Block of Ba^{2+} Currents by Ce, Nd, Gd, Dy, and Yb

The sensitivity of a number of Ca^{2+} -dependent processes on the radius of the metal cation has been investigated by substituting lanthanide cations for Ca^{2+} (reviewed in dos Remedios, 1981). Because the lanthanides have ionic radii close to that of Ca^{2+} , it is thought that the cations with radii closest to that of Ca^{2+} would substitute best for Ca^{2+} at its binding site. On the other hand, lanthanide cations with either larger or smaller ionic radii would be expected to be less effective as a substitute for Ca^{2+} .

To test this prediction, the blocking actions of a series of lanthanide cations that span the series and vary in ionic radius from 0.99 to 1.14 Å were investigated. These values for cationic radius assume an eightfold coordination state. Because cationic radius depends upon coordination number and the coordination numbers for the ions are not known, the radii are used only as a rough guide for comparing the sizes of the different lanthanides (see Shannon, 1976 for discussion).

To determine whether the mechanism of channel block produced by the smaller

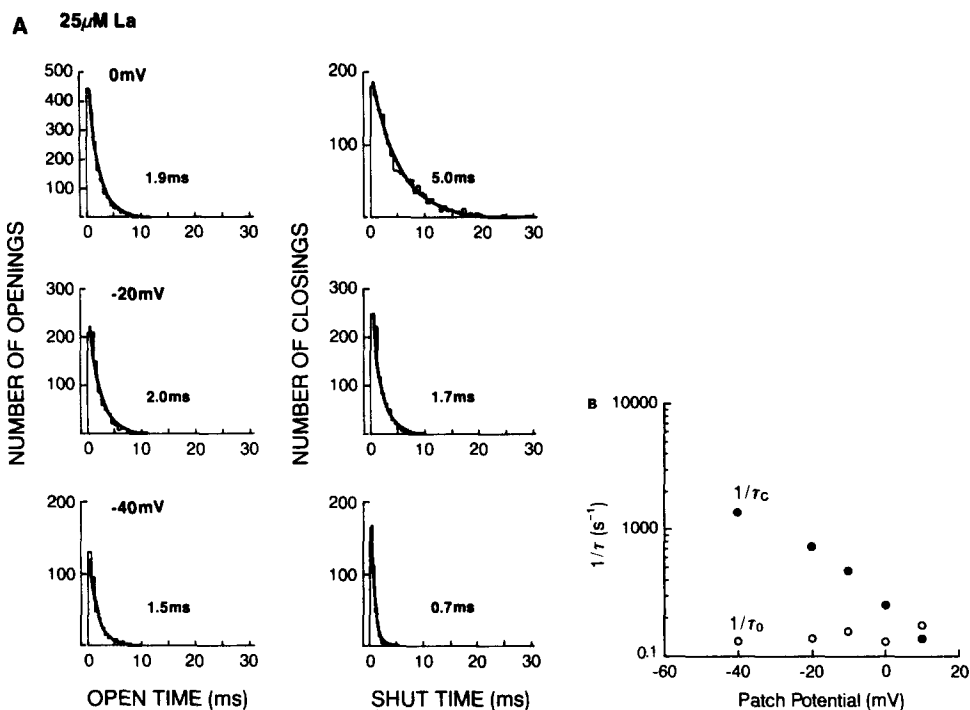


FIGURE 5. Kinetic analysis of the effect of voltage on the block of Ba^{2+} currents by La. (A) Histograms of open and blocked times for the experiment shown in Fig. 4. First column contains the histograms of open times at 0, -20, and -40 mV; second column, the histograms of blocked times. Time constants for the single exponential fits are indicated in the figure. (B) Inverse of mean open time (k_{on}) and mean blocked time (k_{off}) plotted as a function of the patch potential.

lanthanides is similar to La, open and blocked times were measured as a function of the concentration of lanthanide added to the pipette solution and the results were compared with the predictions of the open-channel block model. All of the lanthanides studied produced channel blockade that satisfied the predictions of the model: single exponentials fitted histograms of open and blocked times, the blocking rate depended more or less linearly on blocker concentration, and the rate of unblocking was independent of blocker concentration. The kinetic constants describing

TABLE I
Kinetic Constants for Block of Unitary Ba^{2+} Currents by Lanthanides

Ln	Unhydrated radius*	$g(\text{SD}, n)$	0 mV	-40 mV	0 mV	-40 mV
	\AA	pS	$k_{\text{on}} 10^6 M^{-1} s^{-1} (n)$		$k_{\text{off}} s^{-1} (\text{SD}, n)$	
La	1.16	$14.9 \pm 2.2 (6)$	$13.6 \pm 3.5 (7)$	—	$208 \pm 59 (7)$	$1410 \pm 40 (5)$
Ce	1.14	$13.7 \pm 3.9 (4)$	$4.3 \pm 1.5 (4)$	$7.1 \pm 2.5 (4)$	$85 \pm 22 (4)$	$505 \pm 215 (4)$
Nd	1.11	$14.4 \pm 1.5 (4)$	$2.9 \pm 1.0 (6)$	$2.7 \pm 2.0 (4)$	$38 \pm 10 (6)$	$317 \pm 94 (4)$
Gd	1.05	$14.5 \pm 2.4 (5)$	$3.2 \pm 1.5 (6)$	$5.6 \pm 3.5 (4)$	$34 \pm 13 (6)$	$215 \pm 43 (4)$
Dy	1.03	16.8	$0.7 \pm 0.7 (3)$	—	$34 \pm 11 (3)$	92 (1)
Yb	0.99	$16.0 \pm 1.7 (4)$	$0.5 \pm 0.2 (4)$	0.2 (3)	$21 \pm 6 (4)$	$107 \pm 43 (3)$

Values are \pm SD, and the number of patches is in parentheses.

*Eightfold coordination, Shannon (1976).

channel blockade produced by the lanthanides studied were determined and the results from these experiments are summarized in Table I.

Fig. 6 shows the pattern of block produced by four of the lanthanides studied whose cationic radii range from 1.03 to 1.14 \AA . At 0 mV, 10 μM Ce (1.14 \AA), 10 μM Nd (1.11 \AA), 50 μM Gd (1.05 \AA), and 50 μM Dy (1.03 \AA) produced ~54, 54, 77, and 67% block, respectively; at -40 mV, they produced ~29, 25, 44, and 57% block,

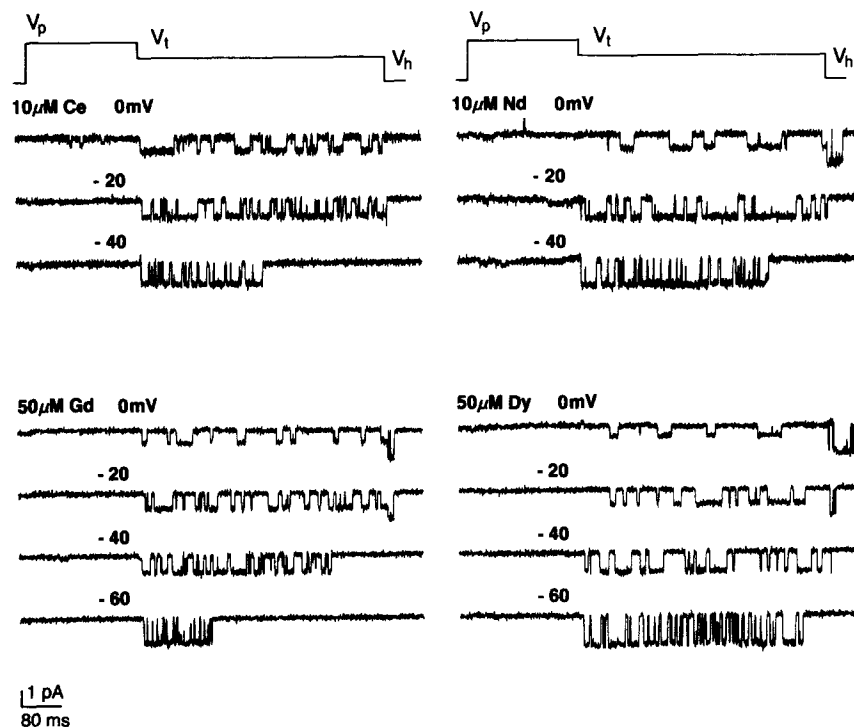


FIGURE 6. Block of unitary Ba^{2+} currents by Ce, Nd, Gd, and Dy. Each set of records is from a different experiment with the indicated concentration of lanthanide added to the 110 mM BaCl_2 electrode filling solution. Currents at each potential were recorded after a depolarizing prepulse of +30 to +50 mV.

indicating that reduction of steady-state block in response to hyperpolarizing the membrane potential is a general characteristic of channel blockade produced by the lanthanides.

Progressing through the series from the larger to smaller cations, the increase in the mean blocked time is particularly clear at -40 mV. Gd (Fig. 6), for example, produces blockages at -40 mV which are quite long when compared with those produced by La (Fig. 4) or Ce (Fig. 6). This effect is not likely to represent an artifact associated with cell-to-cell variations in membrane potential because the unitary current in recordings from different cells at each membrane potential was roughly the same.

The concentration dependence of the mean open time for each of the lanthanides

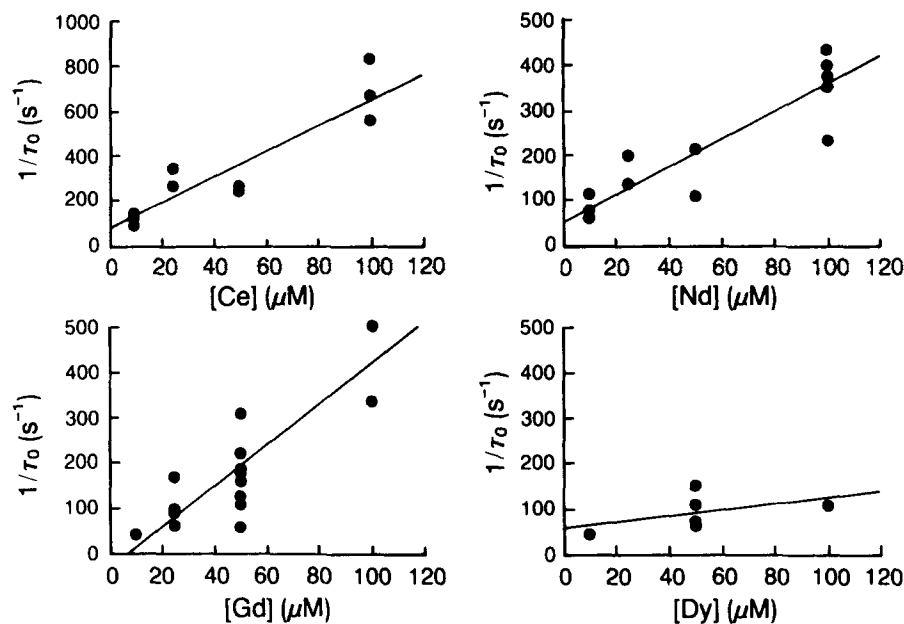


FIGURE 7. Dependence of the inverse of the mean open time on the concentration in the patch electrode of the indicated lanthanide. Straight lines through the experimental points represent the best-fit linear regression lines. Pooled data include results at different test potentials. Number of individual patches indicated in Table I.

studied is shown in Fig. 7 (note the different scales on the ordinates). The inverse of the mean open time depended on the concentration of lanthanide in the patch electrode. The scatter in the relationship between lanthanide concentration and the inverse of the mean open time likely represents variability in the actual concentration of free lanthanide at the membrane surface. The observations that open and blocked times were well fit with single exponentials (data not shown) and that mean blocked times were independent of the concentration of blocker over a wide range of concentrations (Fig. 8, legend), suggest the blocking model holds and that there are not likely to be major kinetic modifications of the channel induced by any of the lanthanides.

Voltage Dependence of Block by Various Lanthanides

For all the lanthanides tested, hyperpolarizing the membrane potential caused the single-channel current to flicker on and off more rapidly. The inverse of the mean blocked times is plotted as a function of membrane potential in Fig. 8. Blocked times depended strongly on membrane potential as shown in Fig. 8. The absolute values of the mean blocked times differed for each of the lanthanides tested (Table I), however, the slopes of the relation between the inverse of the mean blocked time and membrane potential were not significantly different (Fig. 8, legend).

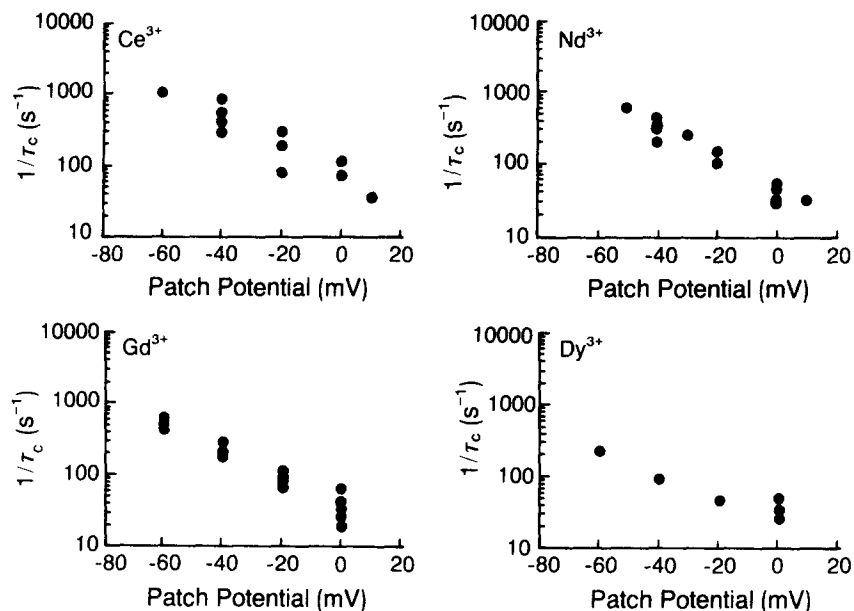


FIGURE 8. Effects of membrane potential on the inverse of the mean blocked time, k_{off} , for Ce, Nd, Gd, and Dy. Each point at each membrane potential represents data obtained from a different experiment. The rate of unblocking changed with hyperpolarization $\sim e$ -fold per 22 mV for Ce ($n = 4$, $r^2 = 0.86$), 19 mV for Nd ($n = 4$, $r^2 = 0.95$), 22 mV for Gd ($n = 6$, $r^2 = 0.94$), 33 mV for Dy ($n = 2$, $r^2 = 0.91$), and 25 mV for Yb (not shown, $n = 4$, $r^2 = 0.88$).

Effects of Ionic Radius on Block of Ba^{2+} Currents by Various Lanthanides

Figs. 9 and 10 summarize the influence of lanthanide cationic radius on the individual steps of blocking and unblocking. The entry rate, k_{on} , for the various lanthanides is plotted as a function of the inverse of ionic radius in Fig. 9. Fig. 9 shows that the entry rate decreased by almost two orders of magnitude across the series. The experimental uncertainties associated with knowing the concentration of free ion in physiological solutions (see Materials and Methods) makes it difficult to draw definite conclusions regarding the absolute value of the entry rate for any given lanthanide. Yet the overall pattern is one in which there is a more or less monotonic decrease in entry rate as one progress through the series.

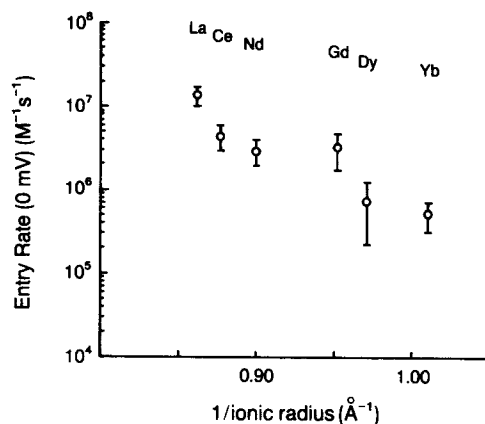


FIGURE 9. Variation of the entry rate, k_{on} , with inverse of cationic radius ($1/\text{\AA}$). The error bars represent the extreme excursion of the least-squares regression line through the data points obtained by "rocking" the line through the maximum and minimum data points while keeping the point at the ordinate fixed.

Fig. 10 shows the exit rate, k_{off} , at two membrane potentials (0 and -40 mV) plotted as a function of the inverse of the cationic radius. Because blockages produced by the smaller lanthanides were so long at 0 mV, it was possible the measured blocked times could be in error in patches containing more than one channel, because it would be easy to miss simultaneous channel openings. At -40 mV , blocked times are short enough to detect multiple channel openings. The relationship between exit rate and cationic radius at both 0 and -40 mV shows a steep decrease from La through Nd, which becomes shallower between Nd and Yb.

DISCUSSION

Relation to Other Work

Since the original observations of Mines (1910) that La and Ce inhibit contraction of the isolated frog heart, trivalent lanthanide cations have been shown to inhibit excitation-contraction coupling of cardiac (Sanborn and Langer, 1970) and smooth muscle (van Breeman, 1969; Mayer et al., 1972; Triggle and Triggle, 1976), as well as transmitter release from neuromuscular synapses (Miledi, 1971; Alnaes and Rahamimoff, 1974; Curtis et al., 1986), and K^+ -stimulated $^{45}\text{Ca}^{2+}$ uptake into brain

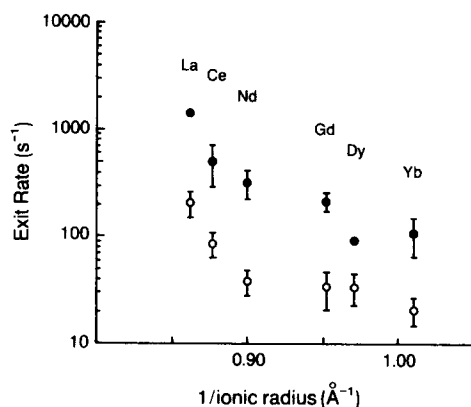


FIGURE 10. Variation of the exit rate, k_{off} , at two membrane potentials (0 and -40 mV , open and filled symbols, respectively) with the inverse of cationic radius ($1/\text{\AA}$).

synaptosomal membranes (Nachsen, 1984). The trivalent lanthanide cations have been assumed to inhibit Ca^{2+} influx through voltage-gated Ca^{2+} channels.

The work described here confirms at the single-channel level that La and other trivalent lanthanide cations are potent inhibitors of currents carried by dihydropyridine-sensitive Ca^{2+} channels in skeletal muscle. Inhibition of Ca^{2+} channel current by the lanthanides arises from the slow rate of dissociation of blocker from the channel, which ranges from $\sim 200 \text{ s}^{-1}$ for La to $\sim 20 \text{ s}^{-1}$ for Yb at 0 mV in the presence of 110 mM BaCl_2 . The rate of La dissociation from the skeletal muscle Ca^{2+} channel is the same, within experimental error, as that measured for the larger conductance channel in cardiac muscle under similar experimental conditions ($\sim 250 \text{ s}^{-1}$, Lansman et al., 1986).

Mechanism of Block

Channel blockade produced by the lanthanides depends strongly on membrane potential and can be relieved by hyperpolarizing the membrane potential. The voltage-dependence of channel blockade is the result of a voltage-dependent increase in the rate of blocker dissociation from its channel binding site. The fact that hyperpolarizing the membrane potential relieves channel blockade produced by all of the lanthanides suggests that the lanthanides are able to traverse the channel and exit into the interior of the cell. The lanthanides, therefore, resemble Cd^{2+} (Byerly et al., 1985; Lansman et al., 1986) as well as Ca^{2+} itself, which blocks monovalent cation currents through the Ca^{2+} channel (Kostyuk et al., 1983; Almers and McCleskey, 1984; Hess and Tsien, 1984; Fukushima and Hagiwara, 1985; Lansman et al., 1986), in being permeant channel blockers.

The sensitivity of blockade to membrane potential, therefore, is most simply explained as the movement of the blocker under the influence of the membrane field, as predicted by a simple model of voltage-dependent channel blockade (Woodhull, 1973). On the other hand, repulsion between permeant ion and blocker within the pore could account for the voltage dependence of channel block if more than one ion at a time can occupy the pore (Almers and McCleskey, 1984; Hess and Tsien, 1984). According to this mechanism, increased occupancy of the pore by the permeant ion Ba^{2+} at negative membrane potentials would speed the exit of the blocking ion from the channel. Further experiments are necessary to distinguish between these two mechanisms.

The blockade produced by all of the lanthanides studied showed roughly the same dependence on membrane potential in which the exit rate increased $\sim e$ -fold per 23 mV of hyperpolarization. It is likely that the blocking particle at physiological pH is the trivalent species, but it is not possible to rule out that the divalent hydroxide or higher valence species contribute to the blocking reaction. If this were the case, however, the sensitivity of block to voltage would be expected to change across the series with the change in the relative proportion of the various charged species in solution. To obtain the same voltage-dependence for the exit rates, it would be necessary to postulate that each charged species experiences a different fraction of the applied voltage, and that the products of cation charge and effective electrical distance sum to an identical value for each of the lanthanides. The simplest conclusion

is that the blocking particle valence remains constant across the series and is either the divalent or trivalent species.

The rate of entry of each of the lanthanides into the Ca^{2+} channel pore was found to be insensitive to membrane potential. The primary transition state for ion entry, therefore, lies outside the membrane field. In having a voltage-independent entry rate, channel blockade produced by the lanthanides resembles the block produced by both Ca^{2+} and Cd^{2+} in cardiac muscle (Lansman et al., 1986). That entry rates are rapid and insensitive to membrane potential is consistent with the idea that the rate-limiting step for the entry of lanthanides into the pore is their rate of diffusion in free solution, a process expected to lie outside the membrane field. In support of this idea, measurements of water substitution rates show that Ca^{2+} , Cd^{2+} , and the lanthanides dehydrate rapidly in aqueous solution and water loss at the inner hydration sphere is the rate-limiting step for complex formation (Diebler et al., 1969).

The effect of cationic radius on the absolute magnitude of the entry rates of the various lanthanides can be compared with the data reported by Diebler et al. (1969) from temperature-jump measurements of lanthanide complex formation with murexide, a Ca^{2+} absorbance indicator. Second-order rate coefficients for La, Ce, and Nd association with murexide are roughly the same ($\sim 10^8 \text{ M}^{-1}\text{s}^{-1}$) and then decrease monotonically across the series reaching a minimum at Yb ($\sim 2 \times 10^7 \text{ M}^{-1}\text{s}^{-1}$). This contrasts with the results presented here which show a much more pronounced decrease in the rate of lanthanide entry into the Ca^{2+} channel pore (Fig. 9).

The difference between the absolute rates of lanthanide association with murexide and entry into the Ca^{2+} channel pore can only partially be accounted for by competition between the permeant ion Ba^{2+} and blocker for a channel site, which would be expected to reduce by about the same amount the entry rate for each of the lanthanides from the maximum diffusion-controlled limit. Some of the reduction of entry rate with ion size may be attributed to more extensive hydrolysis of the smaller ions at physiological pH. The problems with controlling the free lanthanide concentration in the experimental solutions do not allow definite conclusions to be drawn concerning the size dependence of the entry rates beyond the qualitative generalization that they conform to the simple expectation that the smaller ions enter the pore more slowly than the larger ions.

Lanthanide dwell times within the channel differ from the rates of ion entry in their dependence on cationic radius (Fig. 10). The blocked time data show there is a marked reduction in exit rate associated with the reduction in ion size upon moving from La to Nd in the first part of the series. Progressing further through the series, however, there is only a small increase in the stability of interaction between ion and channel binding site. The fact that blocked times vary little with ion size for lanthanides smaller than Nd suggests exit rates may not be determined solely by simple electrostatic interactions with the channel binding site.

The lanthanides, like Ca^{2+} , have flexible coordination numbers and form predominantly ionic complexes which minimize the steric requirements of the ligand (Moeller et al., 1965; Sinha, 1976). The steep decrease in the rate of lanthanide exit from the channel with ion size in the first part of the series and the rather shallow dependence on ion size for the smaller lanthanides may reflect a change in

coordination number. Since ionic radius increases with coordination number, a change in coordination number could help the smaller ions maintain optimal bond lengths with pore ligands (Martin and Richardson, 1979).

An alternative view is that the rate of lanthanide exit from the pore reflects the spacing of charged groups within the pore involved in ion transfer. A large ion may interact more readily with sequentially arranged charged groups as it moves through the pore if the distance between groups is smaller than its effective cationic radius. Smaller lanthanides, on the other hand, unable to form effective complexes with widely spaced ligands, move slowly through the pore. The influence of the spacing of charged groups lining the pore on the kinetics of ion transport contrasts with a simple model of size-selectivity arising from the constraints imposed by a rigid binding site.

Implications for the Structure of the Ca^{2+} Channel Pore

Calculation of the apparent dissociation constant, K_D , from the ratio $k_{\text{off}}(0 \text{ mV})/k_{\text{on}}(0 \text{ mV})$ indicates that the lanthanides La, Ce, and Nd bind with roughly equal affinity to the channel pore. On the other hand, Dy and Yb show a somewhat reduced apparent affinity. This is consistent with the results of Nachsen (1984) who showed a reduction in the apparent affinity of the smaller lanthanides in blocking K^+ -stimulated $^{45}\text{Ca}^{2+}$ uptake into brain synaptosomes. The results presented here suggest that the reduced affinity of the smaller lanthanides for the Ca^{2+} channel represents a reduction of the rate of entry relative to the rate of exit from the channel with decreasing ion size (Figs. 9 and 10).

When the affinity of the Ca^{2+} channel for the lanthanides is calculated using the values of the diffusion-limited association rates of Diebler et al. (1969), there is a sharp increase in affinity from La to Nd followed by a smooth decrease in affinity approaching that of La at Yb. A lanthanide affinity sequence showing a maximum near the middle of the series is characteristic for ligands such as acetate as well as the Ca^{2+} binding sites of various enzymes which generally possess one or two carboxylates and several carbonyl donors (see Nieboer, 1975 for discussion).

The selectivity of the site differs from that of EGTA in which the affinity for lanthanides increases monotonically across the series from the larger to smaller ions (Nieboer, 1975) and which is characteristic of the behavior of weak acid sites and nitrogen donors (Williams, 1982). Although the Ca^{2+} channel binding site has previously been compared with EGTA based on its binding selectivity for Cd^{2+} , Ca^{2+} , and Mg^{2+} (Lansman et al., 1986), the structure of the site is likely to be different from EGTA and the affinity of the site for Cd^{2+} and Mg^{2+} reflects the degree of covalency and coordination requirements of their complexes and not electrostatic interactions arising from differences in ion size.

I thank A. Franco, M. Block, C. Haws, P. Slesinger, and Profs. H. Silber and R. J. P. Williams for helpful comments on the manuscript and Dr. U. Rüegg of Sandoz Ltd. for kindly providing (\pm)-202-791.

Supported by the National Institutes of Health, the Muscular Dystrophy Foundation, and a Basil O'Connor Award from the March of Dimes.

Original versions received 21 March 1989 and accepted version received 6 September 1989

REFERENCES

- Almers, W., and E. W. McCleskey. 1984. Non-selective conductance in calcium channels in frog muscle: calcium selectivity in a single-file pore. *Journal of Physiology*. 353:585–608.
- Alnaes, E., and R. Rahamimoff. 1974. Dual action of praseodymium (Pr^{3+}) on transmitter release at the frog neuromuscular synapse. *Nature*. 247:478–479.
- Armstrong, C. M. 1966. Time course of TEA^+ -induced anomalous rectification in squid giant axons. *Journal of General Physiology*. 50:491–503.
- Armstrong, C. M. 1969. Inactivation of the potassium conductance and related phenomena caused by quaternary ammonium ion injected into squid axons. *Journal of General Physiology*. 54:553–575.
- Biedermann, G., and L. Ciavatta. 1961. Studies of the hydrolysis of metal ions. Part 35. The hydrolysis of the lanthanum ion, La. *Acta Chemica Scandinavica*. 15:1347–1366.
- Byerly, L., P. B. Chase, and J. R. Stormers. 1985. Permeation and interaction of divalent cations in calcium channels of snail neurons. *Journal of General Physiology*. 85:491–518.
- Curtis, M. J., D. M. J. Quastel, and D. A. Saint. 1986. Lanthanum as a surrogate for calcium in transmitter release at mouse motor nerve terminals. *Journal of Physiology*. 373:243–260.
- Diebler, H. M., M. Eigen, G. Illgenfritz, G. Maas, and R. Winkler. 1969. Kinetics and mechanism of reactions of main group metal ions with biological carriers. *Pure and Applied Chemistry*. 20:93–115.
- dos Remedios, C. G. 1981. Lanthanide ion probes of calcium-binding sites on cellular membranes. *Cell Calcium*. 2:29–51.
- Fukushima, Y. 1982. Blocking kinetics of the anomalous potassium rectifier of tunicate egg studied by single channel recording. *Journal of Physiology*. 331:311–331.
- Fukushima, Y., and S. Hagiwara. 1985. Currents carried by monovalent cations through calcium channels in neoplastic B lymphocytes. *Journal of Physiology*. 358:255–284.
- Hagiwara, S. 1975. Ca-dependent action potential. In *Membranes: A Series of Advances*. G. Eisenman, editor. Marcel Dekker, New York. 3:359–381.
- Hagiwara, S., and L. Byerly. 1981. Calcium channel. *Annual Review of Neuroscience* 4:69–125.
- Hagiwara, S., and K. Takahashi. 1967. Surface density of calcium ions and calcium spikes in the barnacle muscle fiber membrane. *Journal of General Physiology*. 50:583–601.
- Hague, D. N. 1977. Dynamics of substitution of metal ions. In *Chemical Relaxation in Molecular Biology*. I. I. Pecht and R. Rigler, editors. Berlin: Springer-Verlag, Berlin. 84–106.
- Hamill, O. P., A. Marty, E. Neher, B. Sakmann, and F. J. Sigworth. 1981. Improved patch clamp techniques for high-resolution current recording from cells and cell-free membrane patches. *Pflügers Archiv*. 391:85–100.
- Hess, P., J. B. Lansman, and R. W. Tsien. 1984. Different modes of calcium channel gating behaviour favoured by dihydropyridine Ca agonists and antagonists. *Nature*. 311:538–544.
- Hess, P., J. B. Lansman, and R. W. Tsien. 1986. Calcium channel selectivity for divalent and monovalent cations. Voltage and concentration dependence of single channel current in ventricular heart cells. *Journal of General Physiology*. 88:293–319.
- Hess, P., and R. W. Tsien. 1984. Mechanism of ion permeation through calcium channels. *Nature*. 309:453–456.
- Hille, B. 1984. *Ionic Channels of Excitable Membranes*. Sinauer Associates, Inc., Sunderland, MA. 426 pp.
- Hoshi, T., and S. J. Smith. 1987. Large depolarization induces long openings of voltage-dependent calcium channels in adrenal chromaffin cells. *Journal of Neuroscience*. 7:571–580.
- Inestrosa, N. C., J. B. Miller, L. Silberstein, L. Ziskind-Conheim, and Z. Hall. 1983. Developmental regulation of 16S acetylcholinesterase and acetylcholine receptors in a mouse muscle cell line. *Experimental Cell Research*. 147:393–405.

- Kostyuk, P. G., S. L. Mironov, and Y. M. Shuba. 1983. Two ion-selecting filters in the calcium channel of the somatic membrane of mollusc neurons. *Journal of Membrane Biology*. 76:83–93.
- Lansman, J. B. 1989. Blocking actions of trivalent lanthanide cations on single dihydropyridine-sensitive calcium channels in skeletal muscle cells from the mouse C2 cell lines. *Biophysical Journal*. 55:595a. (Abstr.)
- Lansman, J. B., P. Hess, and R. W. Tsien. 1986. Blockade of current through single calcium channels by Cd^{2+} , Mg^{2+} , and Ca^{2+} . Voltage and concentration dependence of calcium entry into the pore. *Journal of General Physiology*. 88:321–347.
- Linkhart, T. A., C. H. Clegg, and S. D. Hauschka. 1981. Myogenic differentiation in permanent clonal mouse myoblast cell lines: regulation by macromolecular growth factors in the culture medium. *Developmental Biology*. 86:19–30.
- Martin, R. B., and F. S. Richardson. 1979. Lanthanides as probes for calcium in biological systems. *Quarterly Review of Biophysics*. 12:181–209.
- Mayer, C. J., C. van Breeman, and R. Casteels. 1972. The action of lanthanum and D600 on the calcium exchange in the smooth muscle cells of the guinea-pig taenia coli. *Pflügers Archiv*. 337:333–348.
- Miledi, R. 1971. Lanthanum ions abolish the “calcium response” of nerve terminals. *Nature*. 229:410–411.
- Mines, G. R. 1910. The action of beryllium, lanthanum, yttrium, and cerium on the frog's heart. *Journal of Physiology*. 40:327–346.
- Moeller, T., D. F. Martin, L. C. Thompson, R. Ferrus, G. R. Feistel, and W. J. Randall. 1965. The coordination chemistry of yttrium and rare earth metal ions. *Chemical Reviews*. 65:1–51.
- Nachsen, D. 1984. Selectivity of the Ca binding site in synaptosome Ca channels. *Journal of General Physiology*. 83:941–967.
- Neher, E., and J. H. Steinbach. 1978. Local anesthetics transiently block currents through single acetylcholine receptor channels. *Journal of Physiology*. 277:153–176.
- Nieboer, E. 1975. The lanthanide ions as structural probes in biological and model systems. *Structure and Bonding*. 22:1–47.
- Sanborn, W. G., and G. A. Langer. 1970. Specific uncoupling of activation and contraction in mammalian cardiac tissue by lanthanum. *Journal of General Physiology*. 56:191–217.
- Shannon, R. D. 1976. Revised effective ionic radii and systematic studies of interatomic distances in halides and chalcogenides. *Acta Crystallographica*. A32:751–767.
- Sinha, S. P. 1976. Structure and bonding in highly coordinated lanthanide complexes. *Structure and Bonding*. 25:69–149.
- Smith, R. M., and A. E. Martell. 1976. Critical Stability Constants Vol. 4: Inorganic Complexes. Plenum Publishing Co., New York and London. 2–3.
- Tam, S., and R. J. P. Williams. 1985. Electrostatics and biological systems. *Structure and Bonding*. 63:103–150.
- Triggle, C. R., and D. J. Triggle. 1976. An analysis of the action of cations of the lanthanide series on the mechanical responses of guinea-pig ileal longitudinal muscle. *Journal of Physiology*. 254:39–54.
- van Breeman, C. 1969. Blockade of membrane calcium fluxes by lanthanum in relation to vascular smooth muscle contractility. *Archives Internationales de Physiologie et de Biochimie*. 77:710–716.
- Williams, R. J. P. 1982. The chemistry of lanthanide ions in solution and in biological systems. *Structure and Bonding*. 50:80–119.
- Woodhull, A. 1973. Ionic blockage of sodium channels in nerve. *Journal of General Physiology*. 61:687–708.
- Yaffe, D., and O. Saxel. 1977. Serial passaging and differentiation of myogenic cells isolated from dystrophic mouse muscle. *Nature*. 270:725–727.